RESEARCH PAPER

RNA Biology 10:2, 216–227; February 2013; © 2013 Landes Bioscience

d(GGGT)$_4$ and r(GGGU)$_4$ are both HIV-1 inhibitors and interleukin-6 receptor aptamers

Eileen Magbanua,[1,†] Tijana Zivkovic,[1,†] Björn Hansen,[2] Niklas Beschorner,[3] Cindy Meyer,[1] Inken Lorenzen,[4] Joachim Grötzinger,[4] Joachim Hauber,[3] Andrew E. Torda,[2] Günter Mayer,[5] Stefan Rose-John[4] and Ulrich Hahn[1,*]

[1]Institute for Biochemistry and Molecular Biology; Chemistry Department; MIN-Faculty; Hamburg University; Hamburg, Germany; [2]Centre for Bioinformatics; Hamburg University; Hamburg, Germany; [3]Heinrich Pette Institute; Leibnitz Institute for Experimental Virology; Hamburg, Germany; [4]Institute of Biochemistry; Medical Faculty; Christian-Albrechts-University; Kiel, Germany; [5]Life and Medical Sciences Institute; University of Bonn; Bonn, Germany

[†]These authors contributed equally to this work.

Keywords: aptamers, G-quadruplex, interleukin 6 receptor, HIV, gp120, HIV integrase

Abbreviations: SELEX, systematic evolution of ligands by exponential enrichment; TBA, thrombin binding DNA aptamer; IL-6R, interleukin-6-receptor; IL-6, interleukin 6; sIL-6R, soluble human IL-6 receptor; SPR, surface plasmon resonance; RU, response units; CD spectroscopy, circular dichroism spectroscopy; MD simulation, molecular dynamic simulation; RMSD, root-mean-square deviation; LTR, long terminal repeat; FRA, filter retention assay; ODN, oligonucleotide; NHS, N-hydroxysuccinimide; EDC, N-ethyl-N'-(3-dimethylaminopropyl) carbodiimide

Aptamers are oligonucleotides that bind targets with high specificity and affinity. They have become important tools for biosensing, target detection, drug delivery and therapy. We selected the quadruplex-forming 16-mer DNA aptamer AID-1 [d(GGGT)$_4$] with affinity for the interleukin-6 receptor (IL-6R) and identified single nucleotide variants that showed no significant loss of binding ability. The RNA counterpart of AID-1 [r(GGGU)$_4$] also bound IL-6R as quadruplex structure. AID-1 is identical to the well-known HIV inhibitor T30923, which inhibits both HIV infection and HIV-1 integrase. We also demonstrated that IL-6R-specific RNA aptamers not only bind HIV-1 integrase and inhibit its 3' processing activity in vitro, but also are capable of preventing HIV de novo infection with the same efficacy as the established inhibitor T30175. All these aptamer target interactions are highly dependent on formation of quadruplex structure.

Introduction

In 1990, Ellington and Szostak as well as Tuerk and Gold independently described SELEX (systematic evolution of ligands by exponential enrichment)—a method to select aptamers.[1-3] Aptamers are small oligonucleotides that bind target molecules with high affinity and specificity. During the past two decades, numerous aptamers have been selected for a huge variety of targets ranging from small molecules like fluorophores[4] to whole cells[5] or organisms.[6] Aptamers are now of great interest in fields such as diagnostics, therapeutics, biosensing or gene silencing.

Aptamer specificity reflects their three-dimensional structure, the specific arrangement of loops and stems and the hydrogen bonds that stabilize the structure. In guanine-rich aptamers, there are many examples of the slightly less common motif, the G-quadruplex. This consists of layers, each with four guanine nucleotides, held together by Hoogsteen hydrogen bonds and coordinated monovalent cations. G-quadruplexes occur naturally in telomers as well as in promoter regions.[7-10]

Several putative quadruplex-forming DNA and RNA aptamers for therapeutically relevant target molecules have been described, e.g., the thrombin-binding DNA aptamer (TBA),[11] an RNA aptamer (GGA)$_4$ specific for bovine prion protein[12,13] and the ethanolamine-binding DNA aptamer.[14] Recently, we selected AIR-3A,[15] an G-quadruplex-forming RNA aptamer with specificity for the interleukin-6-receptor (IL-6R). Other G-quadruplex-forming aptamers are already in clinical trials. Among these are the nucleolin-binding aptamer AS1411 for acute myeloid leukemia and renal cell carcinoma,[16] which is composed of two DNA oligonucleotides, and Zintevir an aptamer neutralising HIV infection.[17] Zintevir (also known as T30177, **Table 1**) has the sequence 5'-G*TGGTGGGTGGGTGGG*T-3'. In this case, the insertion of two internucleoside phosphorothioates (G*) led to reduced degradation without influencing its inhibitory effect.[18] Zintevir, as well as its unmodified counterpart T30175 (5'-GTGGTGGGTGGGTGGGT-3'), belong to a group of HIV inhibitors, consisting of only deoxy-guanosines and -thymidines.[19] Another derivative of Zintevir with an equal antiviral effect is the structurally more stable inhibitor, T30695 (5'-G*GGTGGGTGGGTGGG*T-3') as well as its unmodified version, referred to as T30923.[17,20] T30695 and T30923 are composed of a remarkable repetitive nucleotide motif:

*Correspondence to: Ulrich Hahn; Email: uli.hahn@uni-hamburg.de
Submitted: 10/11/12; Accepted: 11/18/12
http://dx.doi.org/10.4161/rna.22951

Table 1. HIV inhibitors

G-quadruplex	Sequence (5'-3')
T30177 = Zintevir = AR177	G*TGGTGGGTGGGTGGG*T
T30175	GTGGTGGGTGGGTGGGT
T30695	G*GGTGGGTGGGTGGG*T
T30923 = d(GGGT)$_4$ = AID-1	GGGTGGGTGGGTGGGT

G* = internucleoside phosphorothioates.

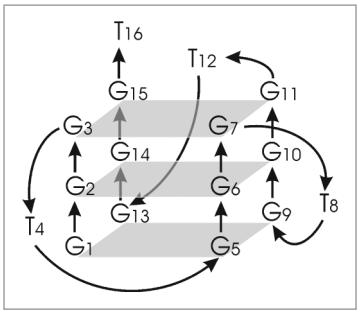

Figure 1. Putative G-quadruplex structure of AID-1. Scheme of parallel-stranded G-quadruplex topology[21,52] with nucleotides consecutively numbered. G1 represents the 5'-end and T16 the 3'-end, respectively.

d(GGGT)$_4$. Surprisingly, two different structures have been reported for d(GGGT)$_4$. On the basis of CD spectroscopy and electrospray ionization mass spectrometry, it has been suggested that d(GGGT)$_4$ forms a parallel-stranded quadruplex with three tetrads in which all guanines are involved (**Fig. 1**).[18,21] In contrast, NMR data with molecular modeling led to an anti-parallel-stranded quadruplex structure[22] with two guanine tetrads. Both structures have in common that coordination of monovalent cations like potassium stabilizes the quadruplex structure.

The inhibitory effect of Zintevir was initially attributed to its inhibition of HIV-1 integrase 3' processing activity,[17] but HIV gp120 was later identified as the primary target, thus preventing interaction with the CD4 receptor, which is essential for HIV infection.[23]

We report here on the selection of IL-6R-specific aptamers. The multifunctional cytokine interleukin 6 (IL-6) and its receptor IL-6R are attractive targets for therapeutic agents as they are associated with diverse diseases such as osteoporosis and rheumatoid arthritis. They are also involved in inflammatory responses as well as in regulation of endocrinal or metabolic mechanisms.[24] The G-quadruplex-forming DNA aptamers selected in this study do not interfere with IL-6/IL-6R interaction. One of these DNA aptamers, AID-1, turned out to have exactly the same sequence [d(GGGT)$_4$] and activity as the HIV-1 inhibitor T30923 mentioned above.

We identified aptamer variants, which affected binding to IL-6R and investigated the effect on quadruplex structure. We then examined the inhibitory effect of IL-6R aptamers and variants with retained or lost quadruplex structure on both HIV integrase activity as well as on HIV infection. Additionally, we tested the RNA aptamer AIR-3A and the RNA counterpart of d(GGGT)$_4$ to this regard.

Results

Selection and identification of DNA aptamers with affinity for the soluble human IL-6 receptor (sIL-6R). After 13 rounds of in vitro selection, five DNA aptamers were identified that recognized sIL-6R. All shared a conserved stretch of 16 nucleotides: 5'-GGGTGGG(T/C)GGGTGGG(T/A)-3'. These guanine-rich DNA aptamers bound sIL-6R with high affinity and binding constants in the low micromolar range (**Table S1**). In addition, the interaction of IL-6R with the cytokine IL-6 and the signal transducer gp130 in the presence of bound AID-27 was analyzed by FRA. Neither the interaction of IL-6R with the cytokine IL-6 nor with gp130 was influenced by bound AID-27 (**Fig. S1**).

The aptamer AID-27 was shortened from both ends to yield AID-1 comprising the conserved 16-base motif d(GGGT)$_4$. Its interactions with its original target (sIL-6R) as well as with the designer cytokine "Hyper-IL-6"[27] were further characterized. Hyper-IL-6 is a fusion protein consisting of sIL-6R and the cytokine IL-6 covalently connected by a poly(Gly-Ser) linker. AID-1 showed a high affinity for Hyper-IL-6 with a K_d of 209 nM (**Fig. 2**). A control FRA measurement with IL-6, thrombin and lysozyme showed no non-specific binding (**Fig. S2**).

The interaction between AID-1 and Hyper-IL-6 was further analyzed by surface plasmon resonance (SPR) measurements to define the association (k_{on}) and dissociation rates (k_{off}). Hyper-IL-6 was immobilized on spot-1 of a carboxymethylated sensor chip using EDC/NHS chemistry. Since IL-6 did not interact with the aptamers (see above), it was immobilized on spot-2 of the same sensor chip to serve as a control. The formation of AID-1/Hyper-IL-6 complexes was monitored as SPR signal given in response units (RU). For all sensorgrams, background RUs from control spot-2 were subtracted from signals on spot-1. As shown in **Figure S3**, the SPR signals of AID-1 binding to Hyper-IL-6 increased in a concentration-dependent manner. Furthermore, the aptamer showed a rapid association and a rapid dissociation as well. The dissociation rate constant (k_{off}) and association rate constant (k_{on}) were determined to be 4.2×10^{-2} $M^{-1}s^{-1}$ and 1.5×10^{4} $M^{-1}s^{-1}$, respectively. AID-1 bound Hyper-IL-6 with a K_d of 490 nM and the K_d determination using SPR and FRA yielded in comparable results.

Hyper-IL-6 binding was also analyzed with variants comprising the repetitive motifs d(GGT)$_4$ and d(GGGGT)$_4$ as well as with the TBA, which solely consists of deoxy guanosines and thymidines. In all cases, only AID-1 significantly bound to Hyper-IL-6 (**Fig. S4**).

Due to the fact that structural stability of AID-1 is highly dependent on the presence of monovalent cations,[41] binding was analyzed in selection buffer as well as in Tris buffer with the addition of potassium or sodium, respectively (**Fig. 3**). Binding to Hyper-IL-6 occurred in all three buffers. But differences regarding proportion of binding could be detected in the buffer containing sodium. As it is known that sodium does not stabilize quadruplex structure as good as potassium, we concluded that Hyper-IL-6 binding is dependent on structural stability.

Affinity of AID-1 variants for Hyper-IL-6. The binding of AID-1 variants was measured by FRA in order to identify sites as important for Hyper-IL-6 binding (**Fig. 2 and Table 2**). AID-1-T, a variant omitting the 3'-terminal thymidine (T16), revealed a dissociation constant of 127 nM being similar to that of AID-1. To analyze whether the other remaining thymidine nucleotides were necessary for Hyper-IL-6 binding, each thymidine was individually replaced by adenosine (AID-1-T4A, -T8A, -T12A, -T16A). Furthermore, all thymidine nucleotides were replaced simultaneously by adenosine yielding AID-1+A. T8A and T12A exchanges had no influence on Hyper-IL-6 binding compared with AID-1 (**Table 2 and Fig. 2B**). Variants T4A and T16A, however, showed reduced affinity and AID-1+A barely bound Hyper-IL-6 (**Table 2**). We then examined the influence of single guanosine to thymidine exchanges within the first G-triplet (AID-1-G1T, -G2T, -G3T). Additionally, four variants were tested in which the first guanine of each of the four remaining G-tetrads was replaced simultaneously (PolyGT) or individually (AID-1-G6T, -G10T, -G14T). Finally, the guanosines of the central tetrad were replaced by adenosines (AID-1-G6A, AID-1-G6A/G14A). FRA showed that all guanosine replacements resulted in a complete loss of Hyper-IL-6 binding activity (**Table 2**).

The RNA counterpart [r(GGGU)$_4$] of AID-1, which we refer to as rAID-1, was tested with respect to Hyper-IL-6 affinity. The measured binding (K_d = 208 nM) was similar to that of AID-1 (**Fig. 2A**). More rAID-1 variants were then analyzed. The deletion of the uracil nucleotide at the 3'-end (rAID-1-U) did not impair binding ability to Hyper-IL-6 (K_d = 199 nM). Further single guanosine transversions within the central tetrad (rAID-1-G2U, -G6U, -G10U, -G14U), however, caused losses in binding capabilities (**Table 2**).

AID-1, here selected as an IL-6R DNA aptamer, turned out to be identical to the known HIV inhibitor T30923.[42] Another HIV-1 inhibitor, T30175, with a similar sequence (5'-GTGGTGGGTGGGTGGGT-3') was analyzed with respect to its binding behavior to Hyper-IL-6 via FRA. T30175 differs in only one additional thymidine nucleotide at position two.[43] FRA revealed that T30175 also bound Hyper-IL-6 (K_d = 293 nM, **Table 2 and Fig. 2A**), but not the cytokine IL-6 itself, indicating its affinity for IL-6R (**Fig. S5**).

Structural analyses of AID-1 and its variants via circular dichroism (CD) and thermal stability experiments. d(GGGT)$_4$ or AID-1 as well as rAID-1, AIR-3A and T30175 have already been shown to exhibit an intrinsic all-parallel G-quadruplex. G-quadruplex formation and thermal stability could be demonstrated by CD spectroscopic analyses and stability tests.[15,20,21,44] The stability of all these quadruplexes was dependent on the presence of monovalent cations. Furthermore, a preference was observed at which potassium ions were favored over sodium ions.

To elucidate the correlation between structural stability and sequence in relation to their functionality, AID-1 variants were analyzed and compared concerning CD spectra and T_m values. All data are summarized in **Table 2**.

The AID-1 aptamer variant AID-1-T showed a significantly increased CD signal at 265 nm (**Fig. 4A**) and retained a T_m value of > 85°C (**Fig. 4C and Table 2**). Thus, removal of 3' thymine (T16) did not destabilize quadruplex formation.[21] Aptamer variants with a thymine nucleotide replaced by adenine (AID-1-T4A, -T8A, -T12A, -T16A, AID-1+A) showed CD spectra characteristic of quadruplex structure with signal strengths comparable to AID-1 (T12A: **Fig. 4C**) and T_m values were slightly reduced (61–80°C). Replacing single deoxy guanosine nucleotides by adenine or thymine nucleotides within the G-tetrad (AID-1-G1T, -G2T, -G3T, -G6T, -G6A -G10T, -G14T) led to destabilization of the

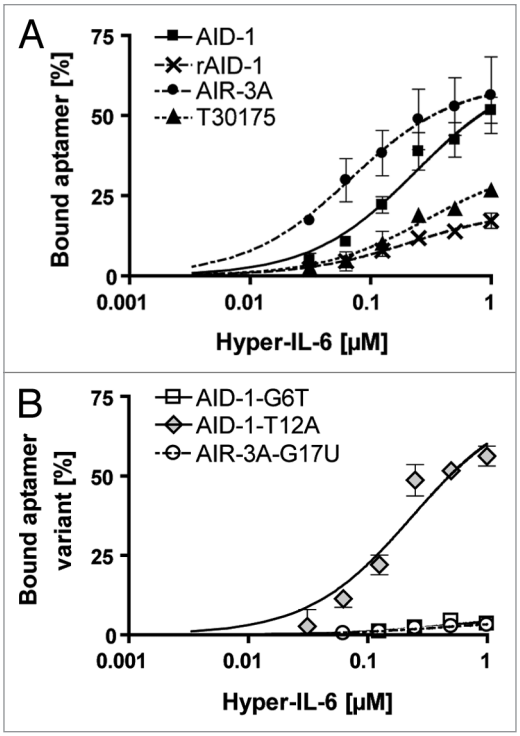

Figure 2. IL-6 receptor-specific aptamers and variants. (**A**) AID-1, rAID-1, AIR-3A and T30175 and (**B**) corresponding variants AID-1-G6T, -T12A and AIR-3A-G17U were incubated with increasing amounts (0–1 μM) of Hyper-IL-6 (**A and B**). Filter retention assays with constant amounts (< 1 nM) of ^{32}P-radioactively labeled aptamers.

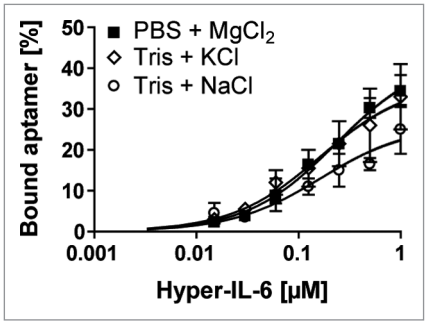

Figure 3. Influence of different monovalent cations on Hyper-IL-6 binding to AID-1. FRA were performed in presence of selection buffer (3 mM $MgCl_2$ in PBS) and Tris buffer (20 mM, pH 7.4) with addition of potassium (100 mM KCl) or sodium (100 mM NaCl), respectively. Filter retention assays with constant amounts (< 1 nM) of ^{32}P-radioactively labeled aptamers.

Table 2. DNA and RNA aptamers as well as their variants with affinity for Hyper-IL-6 are affected regarding quadruplex structure

Oligomers	Sequence (5'-3')	Binding to Hyper-IL-6 K_d (nM)	CD signal[a]	T_m [°C]
AID-1	d(GGGTGGGTGGGTGGGT)	209 ± 96	1	> 85
AID-1-T	d(GGGTGGGTGGGTGGG)	127 ± 79	1.8	> 85
AID-1-G1T	d(**T**GGTGGGTGGGTGGGT)	n.d.[b]	0.6	30
AID-1-G2T	d(G**T**GTGGGTGGGTGGGT)	n.d.	0.7	< 20
AID-1-G3T	d(GG**T**TGGGTGGGTGGGT)	n.d.	0.6	35
AID-1-G6T	d(GGGTG**T**GTGGGTGGGT)	n.d.	0.7	< 20
AID-1-G10T	d(GGGTGGGTG**T**GTGGGT)	n.d.	0.6	< 20
AID-1-G14T	d(GGGTGGGTGGGTG**T**GT)	n.d.	0.6	< 20
AID-1-G6A	d(GGGTG**A**GTGGGTGGGT)	n.d.	0.7	< 20
AID-1-G6A/G14A	d(GGGTG**A**GTGGGTG**A**GT)	n.d.	0.2	< 20
AID-1-T4A	d(GGG**A**GGGTGGGTGGGT)	420 ± 160	1.4	76
AID-1-T8A	d(GGGTGGG**A**GGGTGGGT)	316 ± 59	1.6	74
AID-1-T12A	d(GGGTGGGTGGG**A**GGGT)	234 ± 71	1.3	77
AID-1-T16A	d(GGGTGGGTGGGTGGG**A**)	693 ± 392	1.3	> 80
AID-1+A	d(GGG**A**GGG**A**GGG**A**GGG**A**)	691 ± 271	1.6	61
PolyGT	d(G**T**GTG**T**GTG**T**GTG**T**GT)	n.d.	0.1	< 20
NK3	d(G**TT**TG**T**GT**TT**GTG**T**GT)	n.d.	0.1	< 20
T30175	d(GTGGTGGGTGGGTGGGT)	293 ± 94	0.9	62
d(GGT)$_4$	d(GGTGGTGGTGGT)	n.d.	0.4	n.d.
d(GGGGT)$_4$	d(GGGGTGGGGTGGGGTGGGGT)	n.d.	1.8	71
TBA	d(GGTTGGTGTGGTTGG)	n.d.	-0.2[c]	41
rAID-1	r(GGGUGGGUGGGUGGGU)	208 ± 53	1	> 85
rAID-1-U	r(GGGUGGGUGGGUGGG)	199 ± 65	1.5	n.s.[d]
rAID-1-G6U	r(GGGUG**U**GUGGGUGGGU)	n.d.	0.7	n.s.
AIR-3A	r(GGGGAGGCUGUGGUGAGGG)	82 ± 9	0.8	48
AIR-3A-G17U	r(GGGGAGGCUGUGGUGA**U**GG)	n.d.	0.5	< 20
AIR-3A-G17/18U	r(GGGGAGGCUGUGGUGA**UU**G)	n.d.	0.5	< 20

[a]Relative ellipticity at 265 nm with respect to AID-1 or rAID-1, respectively; [b]n.d., not detectable; [c]anti-parallel-stranded quadruplex; [d]n.s., not specified. K_d values were determined by FRA. Quadruplex structure stability was studied by CD spectroscopy and thermal stability analysis. CD signals at 265 nm are listed and reduced CD signals as well as reduced T_m values indicate a less pronounced quadruplex structure. CD signals are presented as relative values to AID-1 (= 1) and rAID-1 (= 1), respectively. Deletions or substitutions of nucleotides are pointed out in bold.

quadruplex structure, which could be observed by a reduced CD signal at 265 nm and a significant reduction of T_m values to below 30°C. Furthermore, replacing two deoxy guanosine nucleotides simultaneously (AID-1-G6A/G14A: **Fig. 4B**), or rather all guanines of the central tetrad by thymidines (PolyGT), led to total loss of quadruplex characteristics in the CD spectra. r(GGGU)$_4$ or rAID-1 was previously described as a quadruplex-forming oligonucleotide.[44] This was verified by CD profiles (**Fig. 4A**) and melting point determination (**Fig. 4C and Table 1**; T_m > 85°C), which displayed a hypochromic effect typical of parallel quadruplex structure. CD spectra of rAID-1 variants containing a single guanosine transversion within the central tetrad (rAID-1-G6U, -G10U, -G14U) did not significantly change compared with rAID-1 (**Table 2**). The dependence of quadruplex formation on monovalent cations was also analyzed by CD spectroscopy in PBS or 50 mM Tris buffer in the absence and presence of 100 mM KCl or 100 mM NaCl, respectively (**Fig. S6**). The 265 nm signals for rAID-1 plus the variants rAID-1-U and rAID-1-G6U decreased in a buffer dependent manner: PBS > 50 mM Tris, 100 mM KCl > 50 mM Tris, 100 mM NaCl > 50 mM Tris. These findings indicate a higher stability in the presence of K^+ ions compared with Na^+ ions. However, the absence of monovalent cations led to complete loss of structure stability. These findings are in accordance with structural stabilities of AID-1.

MD-simulations to test 3D-structure of selected aptamers. One might expect modeling and simulation to show a structural basis for measured differences in binding affinity. The simulation results, however, were dominated by a different result. Weak binding seemed to reflect poor stability of the quadruplex. To estimate this properly, one would need many folding/unfolding events in the simulations, but this will rarely be observable on the timescale of molecular dynamics simulations. One can obtain a less quantitative estimate from the apparent tendency of the molecule to open and drift away from the initial coordinates. This is best measured with a sliding window approach, continuously measuring the drift. To this end, each

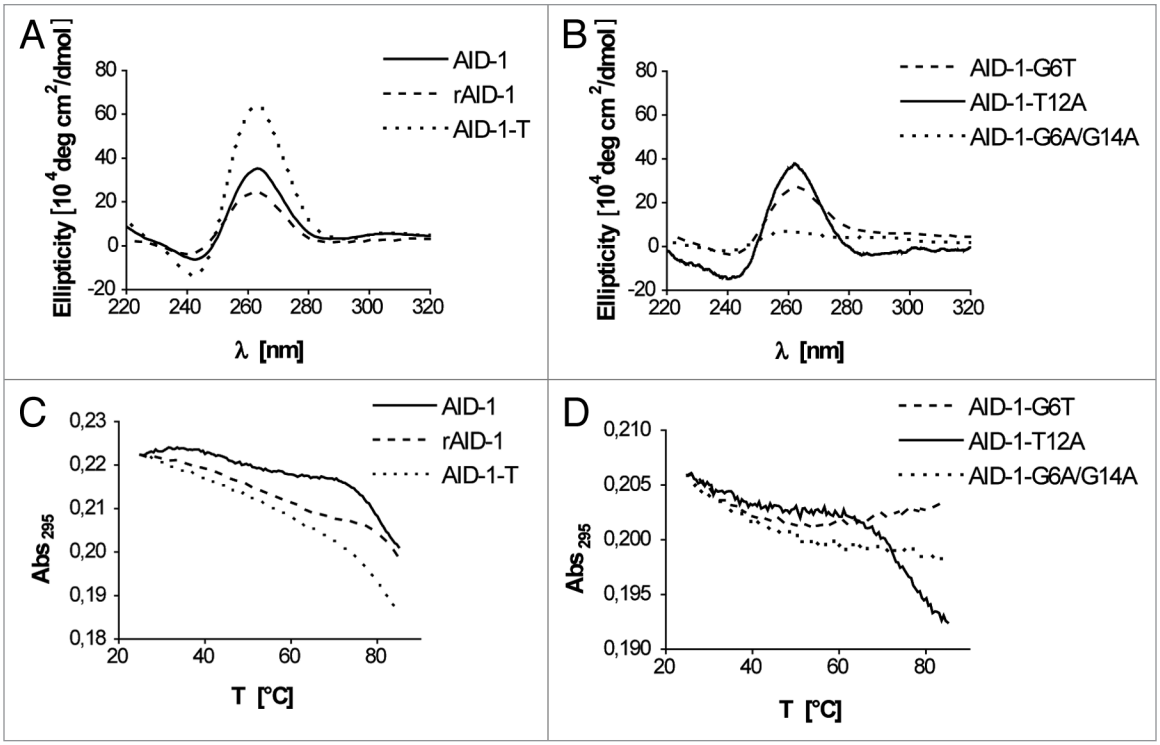

Figure 4. IL-6R aptamer modifications affecting quadruplex structure. (**A and B**) CD spectroscopic analyses in PBS and (**C and D**) melting curves of AID-1, its variants AID-1-T, -G6T, -G6A/G14A, -T12A and the RNA counterpart rAID-1.

snapshot was compared with its counterpart, 2.5 ns earlier in the simulation.

Given this measure, there is no evidence of instability for AID-1 (**Fig. S7**) nor any of the close sequence-related variants: AID-1-G2T, -G6T, -G6A, -G10T or -G14T (AID-1-G6T, see **Fig. S7**). Both the sliding window and absolute rmsd values remain small and comparable with those of AID-1 (0.14 Å ± 0.1). In contrast, variants with several modifications such as PolyGT and NK3 showed significantly increased rmsd values in comparison to AID-1, indicating loss of 3D-stucture (**Fig. 5B**; **Fig. S7**).

We also wanted to verify the quadruplex structure of the rAID-1, the RNA counterpart, using MD simulations. The structure of the DNA aptamer AID-1 served as a template for the initial model. Again, the MD simulation of the RNA aptamer $r(GGGU)_4$ was completely stable over the 35 ns simulation (**Fig. 5A**; **Fig. S7**). Although the simulation shows motions such as the peak around 9 ns (**Fig. S4A**), the rmsd value in the simulations never rose above 1.2 Å, which is even smaller than in the calculations for AID-1. In this particular calculation, one can even explain the major motion. It was due to the 3'-terminal uracil residue detaching itself from the G-quadruplex, which did not disturb the overall structural stability.

Affinity of IL-6R aptamers for HIV-1 integrase and their inhibitory effect on 3' processing activity in vitro. To investigate the affinity of IL-6R aptamers as well as their variants for HIV-1 integrase and their possible inhibitory effects on integrase activity, corresponding FRAs and activity assays were performed. AID-1 and its variants AID-1-G6T and AID-1-T12A bound HIV-1 integrase with affinities in the nanomolar range (K_d values 144 nM, 129 nM and 142 nM, respectively; **Fig. 6A**). AID-1 and AID-1-T12A aptamers showed the same quadruplex structure, but AID-1-G6T showed destabilized structures with T_m values < 20°C (**Fig. 4B and Table 2**). For this reason, a variant, AID-1-G6A/G14A, which showed significantly reduced quadruplex structure (**Fig. 4B**), was analyzed. Despite structural instabilities from CD spectroscopy, AID-1-G6A/G14A bound HIV-1 integrase with a comparable affinity to AID-1 [$d(GGGT)_4$] with a K_d value of 381 nM (**Fig. 6A**). Additionally, we could demonstrate that the IL-6R RNA aptamer rAID-1 as well as the previously described IL-6R RNA aptamer, AIR-3A,[15] and its variant AIR-3A-G17U, which had lost its affinity for IL-6R, still possessed affinity for HIV-1 integrase with K_d values of 151 nM, 20 nM and 8 nM, respectively (**Fig. 6F and Table 3**). All of the tested IL-6R DNA and RNA aptamers as well as their corresponding variants showed comparably high affinities for HIV-1 integrase.

Next, we wanted to see whether HIV-1 integrase binding led to inhibition of HIV-1 integrase activity in vitro. Therefore, we performed activity assays of HIV-1 integrase in the presence of selected DNA or RNA molecules as previously described.[31,32] To investigate 3' processing activity, a radioactively labeled double-stranded DNA served as substrate. During 3' processing, a dinucleotide is cleaved off from the substrate (**Fig. 6C**). Efficiency of the reaction could be monitored by gel electrophoresis (**Fig. 6D**) and the presence of aptamer led to concentration-dependent inhibition of HIV-1 integrase activity. We observed that all aptamers that bound to HIV-1 integrase also influenced its 3' processing activity in a concentration dependent manner (**Fig. 6E and F**). Only the AID-1 variant AID-1-G6A/G14A, which was known

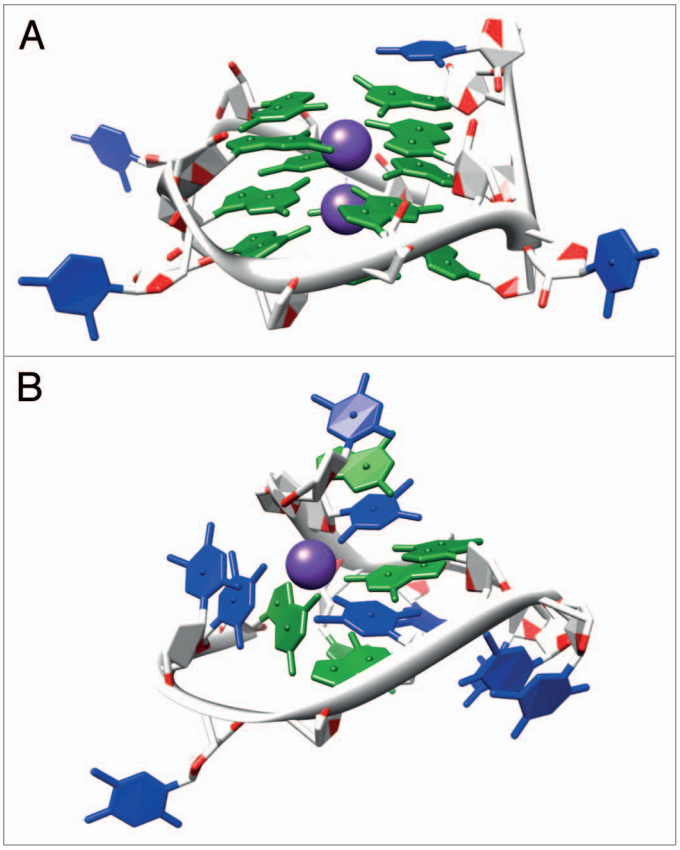

Figure 5. Structures of IL-6R aptamer rAID-1 (**A**) and control aptamer NK3 (**B**) after 35 ns of MD simulation. rAID-1, RNA counterpart of AID-1 (**A**) guanine bases are shown in green, thymine/uracil bases in blue and complexing potassium ions in purple.

to have less quadruplex structure, did not inhibit 3' processing. However, compared with AID-1, the variant AID-1-G6T that had lost the ability to bind IL-6R, inhibited HIV-1 integrase with a 4-fold reduced IC_{50} value of 0.5 mM (**Fig. 6E**). AID-1-T12A, still binding to IL-6R, also served as HIV-1 integrase inhibitor comprising an IC_{50} value of 206 nM (**Fig. 6E and Table 3**).

In addition, the inhibitory effects of the RNA aptamer rAID-1 (the corresponding RNA variant of AID-1) and AIR-3A were analyzed and also turned out to inhibit the 3' processing activity of HIV-1 integrase with IC_{50} values of 49 nM and 74 nM, respectively (**Fig. 6F**). Variants of AIR-3A termed AIR-3A-G17U and AIR-3A-G17/18U, which did not bind the IL-6R, showed three times higher IC_{50} values (149 nM and 193 nM, respectively) in comparison to that of AIR-3A (**Fig. 6F and Table 3**).

To find a possible explanation for the binding of the aptamers to the different proteins, the structures of IL-6R[45] and HIV-1[46] were compared using three programs that detect similarities at the structural level, even without sequence similarity. Neither Salami,[38] Dali[39] nor FATCAT[40] reported any significant structural similarity.

IL-6R aptamers inhibit HIV infection. AID-1 or T30923 and T30175 are well-established HIV infection inhibitors.[17,20] For this reason, we analyzed AID-1, T30175 and, in addition, the IL-6R aptamers rAID-1 and AIR-3A as well as their respective variants (AID-1-G6T, AID-1-G6A/G14A, AIR-3A-G17/18U) for their ability to inhibit HIV de novo infection. For infection of TZM-bl cells,[33] we used the CXCR4-tropic HIV-1 strain NL4/3. Effective infection of TZM-bl cells resulted in activation of HIV-1 long-terminal repeat (LTR) promoter-driven luciferase reporter gene expression. The presence of aptamers during infection process caused a concentration-dependent inhibition of HIV infection, which was detected via reduced luciferase activity (**Fig. 7A–C**). All IL-6R aptamers inhibited HIV infection efficiently at a concentration of 1 μM with exception of the AID-1 variant AID-1-G6A/G14A (**Fig. 7A**: black bars). Again, we could show that aptamer activity is strongly related to its structure. Based on our data, EC_{50} values could be calculated (**Table 4**) and showed that the RNA aptamers rAID-1 and AIR-3A inhibited HIV infection as efficiently as the known inhibitors AID-1 and T30175 with EC_{50} values of 96 and 56 nM, respectively. We also observed that variants with destabilized quadruplex structure inhibited 3-fold (AID-1-G6T) or 95-fold (AID-1-G6A/G14A) less efficiently than the original aptamer.

To exclude a toxic influence of aptamers during infection, cell viability was investigated in parallel. IL-6R aptamers, as well as the known HIV inhibitor T30175, did not affect cell proliferation (data not shown).

Next, we wanted to determine if IL-6R aptamers inhibit HIV infection by blocking interaction with gp120-CD4 as previously described for Zintevir.[23] Therefore, VSV-G pseudotyped HIV-1, lacking the viral envelope proteins, was used for de novo infection experiments. VSV-G pseudotyped virus infected TZM-bl cells by endocytosis independently of gp120. The presence of 1 μM IL-6R aptamer or respective variants did not prevent TZM-bl cells from infection by VSV-G pseudotyped HIV (**Fig. 7A**, white bars). This led to the conclusion that IL-6R aptamers inhibited HIV infection by interfering with the gp120-CD4 interaction. To confirm this, FRA with HIV gp120 was performed. All aptamers bound gp120, although differences were observed regarding binding amplitude. The DNA aptamers T30175 and AID-1 achieved a maximum of binding of 20%, the variant AID-1-G6A/G14A, only 5% which showed least inhibitory effect on HIV infection. The RNA aptamer AIR-3A as well as its variant AIR-3A-G17/18U were completely bound of the protein and their K_d values were equal. Both inhibited HIV infection with same efficiency.

Discussion

The IL-6 receptor aptamer AID-1 and the HIV inhibitor T30923 exhibit the identical sequence, d(GGGT)$_4$. We here report about the selection of a collection of aptamers with high affinities for the IL-6 receptor. One of those selected IL-6R aptamers, d(GGGT)$_4$, also termed AID-1, exhibited a sequence identical to that of an already known HIV inhibitor known as T30923.[42] This derivative of Zintevir (= T30177) interferes with HIV infection in cell culture and inhibits HIV-1 integrase.[17] We could demonstrate that AID-1 bound IL-6R with a K_d value in the nanomolar range and that it was not competing with the cytokine IL-6 for IL-6R or the signal transducer gp130.

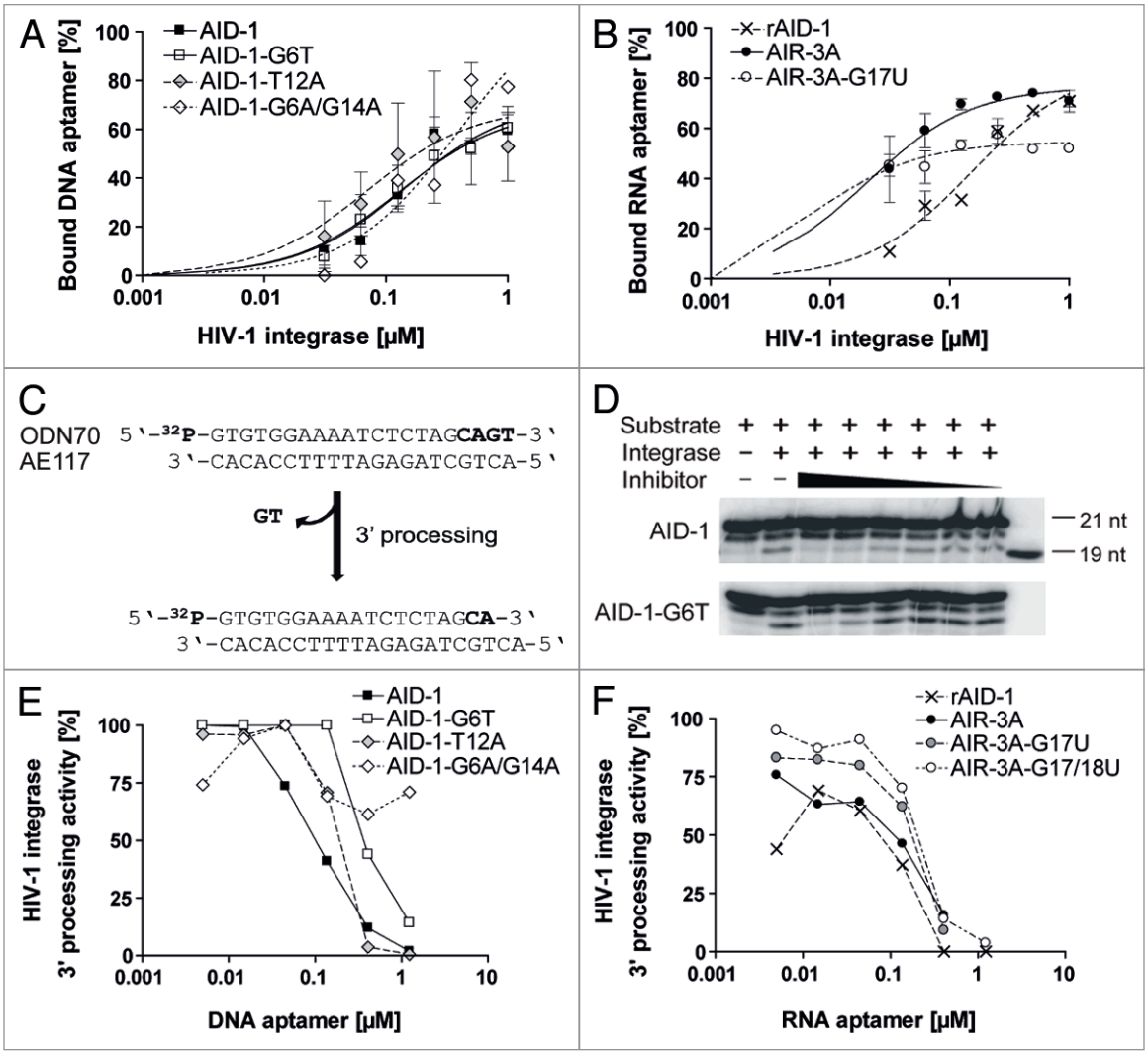

Figure 6. 3' processing activity of HIV-1 integrase and its inhibition by IL-6R aptamers. (**A and B**) DNA, RNA aptamers as well as corresponding variants were incubated with increasing amounts (0–1 μM) of HIV-1 integrase. Binding was detected by using FRA with constant amounts (< 1 nM) of ^{32}P-radioactively labeled aptamers. (**C**) Short oligonucleotides derived from U5 long-terminal repeat DNA ends were used to study 3' processing activity. For this purpose, a 21-mer (ODN70) was radiolabeled with ^{32}P and hybridized to its complementary strand (AE117). ODN70 was converted into a 19-mer oligonucleotide by HIV-1 integrase. (**D**) Gel electrophoresis of reaction was monitored in the presence of increasing amounts (5–1,230 nM) inhibiting AID-1 or its variant AID-1-G6T. (**E and F**) Graph of concentration dependant inhibition of 3' processing activity.

To delineate which single nucleotides of AID-1 are important for IL-6R binding or its structural stability, we also analyzed variants with guanine or thymine nucleotides replaced by thymine or adenine nucleotides, respectively. Regarding IL-6R binding, we identified AID-1 variants possessing thymine transversions that were tolerated. In contrast, guanine transversions or transitions were not tolerated at all (**Table 2**).

Due to the fact that the selected IL-6R aptamer had an identical sequence as an HIV inhibitor, we analyzed other HIV inhibitors for IL-6R binding that had parallel stranded quadruplex structure in common. We found that the published HIV inhibitor T30175, with an additional thymine nucleotide at position two (compared with AID-1), was also able to bind IL-6R in a nanomolar range. But $d(GGGGT)_4$ with proven inhibitory effect on HIV integrase activity[20] did not bind IL-6R. Consequently,

Table 3. Aptamers with affinity for HIV-1 integrase as well as their inhibitory effect on HIV-1 integrase 3' processing activity in vitro

Oligomers	HIV-1 integrase	
	K_d [nM][a]	IC_{50} [nM][a]
T30175	15 ± 8	37
AID-1	144 ± 54	115
AID-1-G6T	129 ± 68	495
AID-1-T12A	140 ± 50	206
AID-1-G6A/G14A	381 ± 244	n.d.[b]
rAID-1	151 ± 32	49
AIR-3A	20 ± 6	74
AIR-3A-G17U	8 ± 4	149

[a]K_d and IC_{50} values were determined based on FRA and HIV-1 integrase activity, respectively. [b]n.d. = not detectable.

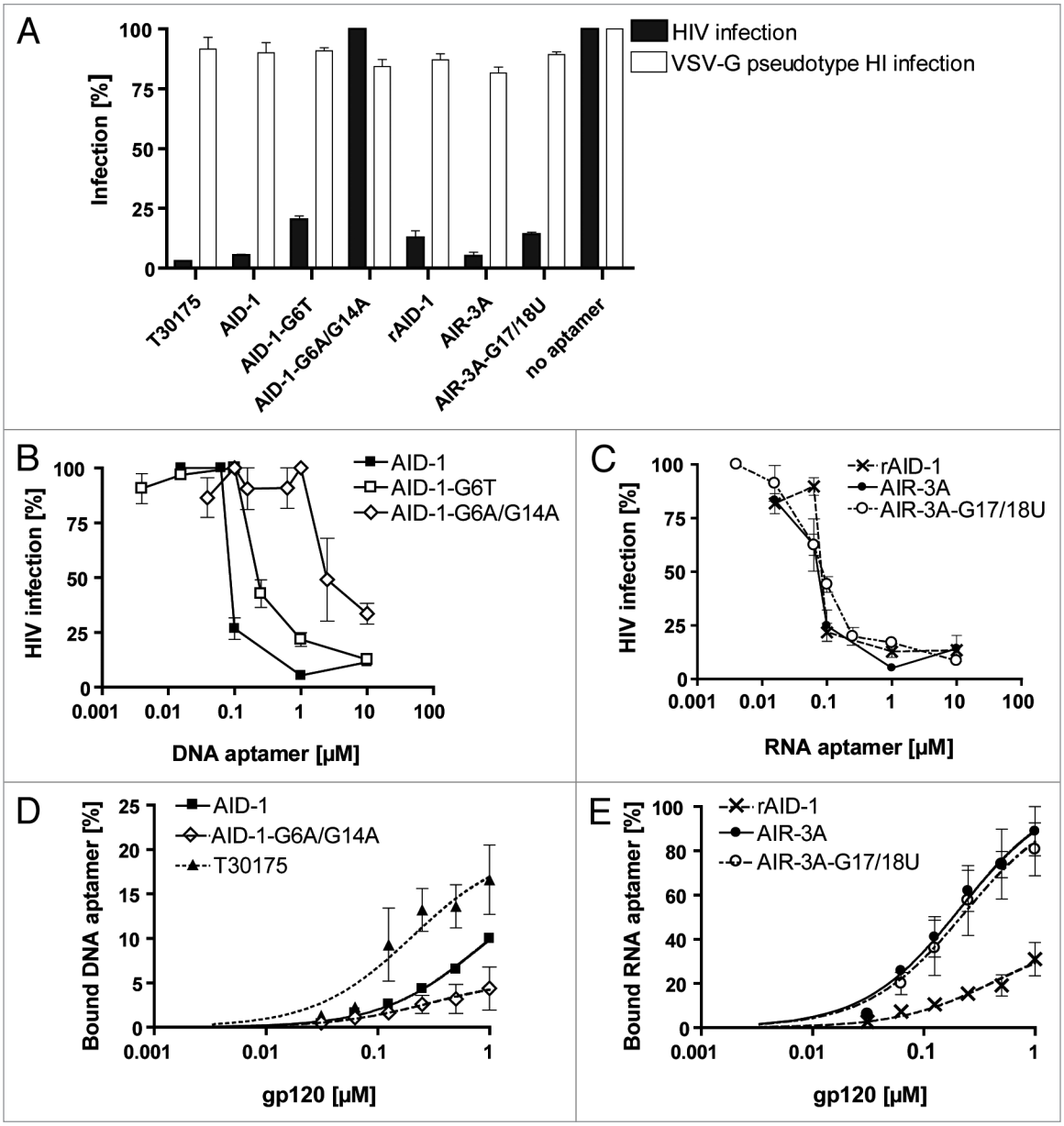

Figure 7. IL-6R aptamers inhibit efficient HIV infection. (**A**) TZM-bl cells were infected by a CXCR4-tropic HI virus (NL4/3; black bars) or a VSV-G pseudotyped HI virus (white bars) in presence of 1 μM IL-6R aptamer. (**B and C**) Aptamers or it variants prevented TZM-bl cells from NL4/3 infection, dependent on concentration (16 nM–10 μM). Effective infection was observed by increasing luciferase activity. (**D and E**) IL-6R DNA and RNA aptamers as well as their variants were incubated with increasing amounts of HIV gp120 (0–1 μM). Binding was detected by FRA using constant amounts (< 1 nM) of ^{32}P-radioactively labeled aptamers.

an additional thymine nucleotide at position two was tolerated for IL-6R binding, but an additional guanine tetrad was not.

Variant analyses revealed that aptamer binding coincided with quadruplex structure formation. CD spectroscopy, thermal stability tests and simulations showed that most of the AID-1 variations led to a destabilization or destruction of the quadruplex structure. Both data from CD spectra and the hypochromic effect seen in melting analyses provided strong evidence for quadruplex structures. Although CD spectra of the variants with single guanines replaced suggested quadruplex structure, the reduced signals at 265 nm, melting behavior and changes of T_m values unequivocally confirmed quadruplex destabilization. More than one guanine replacement, however, led to significantly differing CD spectra.

The MD simulations supported the interpretation of many results in terms of stability, although they are less conclusive than spectroscopy. Only the most destabilizing variants (Poly GT and NK3) were clearly recognized as unstable.

The DNA aptamer AID-1 and its RNA version rAID-1 exhibit equal structure and function. Comparing the aptamers AID-1 and rAID-1, it seems that most results from DNA apply to the RNA analog. CD spectroscopy and thermal stability

measurements confirmed a parallel-stranded quadruplex structure for rAID-1 that was stabilized by monovalent cations with a possible preference for K^+ over Na^+ ions. The findings agree with results of Joachimi et al.,[44] who compared quadruplex-forming DNAs with corresponding RNAs and demonstrated that RNA variants of all-parallel DNA quadruplexes possess the same structures and similar thermal stabilities. The MD simulations showed no differences in stability and the binding measurements showed that rAID-1 is an IL-6R aptamer with affinity as strong as AID-1. Performing the same guanine transversions on rAID-1 and AID-1 led to a similar loss of IL-6R binding. The findings demonstrate that, contrary to general opinion, function and, hence, tertiary structure of DNA can be completely fulfilled by its RNA analog, which so far was only reported twice.[47,48]

Quadruplex structure is also a prerequisit for effective HIV inhibition. To identify aptamer variants with either affinity for IL-6R or HIV integrase, we investigated the binding behavior of the already mentioned variants to HIV-1 integrase and their capacity to inhibit its 3' processing activity in vitro. We could clearly reproduce such an inhibitory effect of AID-1[42] with an IC_{50} value in the nanomolar range. Additionally, IL-6R binding aptamers (rAID-1, AIR-3A) and their variants also showed an inhibitory effect. Differences in inhibition effects, however, could be observed between variants that did bind the IL-6R (AID-1-T12A) and variants that did not (AID-1-G6T, -G6A/G14A, AIR-3A-G17U, -G17/18U). Variants with at least one guanine nucleotide exchange and corresponding structural instabilities lost their affinity for the IL-6R and also exhibited a less inhibitory effect on HIV-1 integrase. These findings indicate that aptamer-protein-interaction is highly associated with stable G-quadruplex formation, which comprises the binding scaffold. Jing et al.[42] already demonstrated for 21 derivatives of AID-1 that there was a functional correlation between thermal stability and the ability to inhibit HIV-1 integrase activity.

In our study, aptamer variants that either bound IL-6R or inhibited HIV-1 integrase could not be identified, probably due to the fact that quadruplex structure is required for the interaction with both proteins.

Furthermore, it should be mentioned that intrinsic, all-parallel quadruplexes inhibit HIV-1 integrase activity in vitro as demonstrated for AID-1, T30175 and $d(GGGGT)_4$[20,21,43] and revealed here for rAID-1 and AIR-3A as well. In contrast, TBA comprising an anti-parallel quadruplex structure did not inhibit HIV-1 integrase.[17]

Structural comparison of IL-6R and HIV integrase did not lead to an explanation for aptamer binding to the two targets. Since IL-6R-binding aptamers inhibit HIV-1 integrase in vivo, one might expect some similarity between the protein targets, but this is not the case. Not only is there no significant sequence similarity, but none of the three programs which look for structural similarity could generate a structural superposition. There are two possible explanations. First, the two different protein folds could still present functional groups in similar orientations in space, albeit from different scaffolds. Second, it is possible that the proteins bind to different sites on the aptamers and there is no similarity in binding modes. Ultimately, this kind of structural question will only be answered by studies of the aptamer-protein complexes.

Table 4. Aptamers inhibiting HIV infection by binding HIV gp120

Oligomers	HIV infection	HIV gp120 binding	
	EC_{50} (nM)	K_d (nM)	Bmax (%)
T30175	56 ± 15	201 ± 111	20 ± 4
AID-1	96 ± 34	775 ± 162	17 ± 2
AID-1-G6T	313 ± 20	n.s.[a]	n.s.
AID-1-G6A/G14A	9120 ± 11	440 ± 60	10 ± 1
rAID-1	45 ± 17	430 ± 220	42 ± 10
AIR-3A	29 ± 10	227 ± 58	100 ± 11
AIR-3A-G17/18U	80 ± 9	230 ± 98	100 ± 17

[a]n.s., not specified. K_d and EC_{50} values were determined based on FRA and inhibition of infection of TZM-bl cells by NL4/3, respectively.

IL-6R RNA aptamers inhibited HIV infection as effective as T30175. It has been reported that T30175 is an efficient HIV inhibitor.[17] This work showed that the IL-6R RNA aptamers, rAID-1 and AIR-3A, are also effective inhibitors of HIV infection and the inhibition seems to be very dependent on quadruplex formation.

T30175 interferes with CD4-gp120 interactions by binding to HIV gp120.[23] The results here showed that IL-6R aptamers AID-1, rAID-1 and AIR-3A were not able to inhibit HIV infection if gp120 was absent. This suggests that IL-6R aptamers inhibit HIV infections in a manner similar to T30175.

Materials and Methods

Chemicals and buffers. Unless otherwise stated, all chemicals were purchased from Sigma-Aldrich and oligonucleotides from Invitrogen.

Proteins. All standard enzymes for molecular biology were obtained from Fermentas, hIL-6 from Merck, HIV-1 integrase from Biocat, HIV gp120 from Sino Biological, Thrombin from CellSystems and Lysozyme from Carl Roth. T7 RNA polymerase,[25] sIL-6R[26] and Hyper-IL-6[27] were isolated from recombinant overproducers as described.

In vitro selection of DNA aptamers. SELEX was performed as previously described.[1] The soluble part of the IL-6 receptor (sIL-6R) was biotinylated using EZ-Link Sulfo-NHS-LC-Biotin reagent (Thermo Fisher Scientific) and coupled to streptavidin-coated magnetic beads (Dynabeads M-280; Thermo Fisher Scientific).[28] The SELEX process was initiated by incubation of the DNA library D1 (5'-GCCTGTTGTGAGCCTCCTAAC-N_{60}-CATGCTTATTCTTGTCTCCC-3', 500 pmol, 3×10^{14} individual molecules), with sIL-6R immobilized on magnetic beads in selection buffer. After extensive washing, remaining DNAs were eluted by heating and amplified via PCR. After 13 SELEX rounds, the resulting dsDNA library was cloned into the vector pUC19. Individual clones were identified by DNA sequencing.[29]

Filter retention assay (FRA). To analyze aptamer-protein interactions, DNA or RNA molecules were terminally

radioactively labeled using T4 polynucleotide kinase and γ-(^{32}P)-ATP (3,000 Ci/mmol; Hartmann Analytic). To perform FRAs with Hyper-IL-6 or HIV gp120, the target protein was serially diluted (0–1 μM) in selection buffer (PBS, 3 mM $MgCl_2$, pH 7.4). For FRAs with HIV-1 integrase, IN buffer [20 mM Hepes, pH 7.5, 10 mM DTT, 7.5 mM $MnCl_2$, 10 mM NaCl, 0.05% (v/v) Nonidet P40] was used. After incubation of the protein with constant amounts of labeled nucleic acids (< 0.5 nM) for 30 min at 37°C, samples were passed through a pre-equilibrated nitrocellulose membrane (0.45 μm, Carl Roth) under vacuum (Minifold I Dot-Blot-System; Schleicher and Schuell, VWR International). After washing twice with buffer, the membrane was dried and exposed to a phosphor-imaging screen (Bio-Rad). The retained radioactivity was quantified using Quantity One software (Bio-Rad).

Circular dichroism (CD) spectroscopy. Quadruplex formation of nucleic acids was measured by CD spectroscopy[30] with a Spectrometer Model 215 (Aviv Biomedical). Samples were prepared with 5 μM DNA or RNA diluted in PBS or 50 mM Tris-HCl, pH 7.4 in presence of 100 mM KCl or NaCl, respectively. Spectra were scanned twice from 200–320 nm at 25°C.

UV spectroscopy. For melting point (T_m) determination, aptamers (2.5 μM) were dissolved in 100 mM Tris-HCl, pH 7.4 and 5 mM KCl. Measurements were performed with a Varian Cary Bio 300 UV-Visible Spectrophotometer. Aptamer solution was then transferred into a quartz cuvette (1-cm path length) and covered with mineral oil. Heating and subsequent cooling were performed in steps of 0.5°C min^{-1} between 20–85°C. Absorption was monitored at 295 nm. T_m values were calculated based on the van't Hoff equation.

HIV-1 integrase-inhibiting assay. Aptamer inhibition of 3' processing activity of HIV-1 integrase was determined as previously described.[31,32] Oligonucleotides (ODN) derived from the U5 end of the HIV long-terminal repeat were the following: ODN70 d(GTGTGGAAAATCTCTAGCAGT), ODN71 d(GTGTGGAAAATCTCTAGCA)[31] and AE117 d(ACTGCTAGAGATTTTCCACAC).[32] ODN70 was radioactively labeled with T4 polynucleotide kinase and hybridized to AE117 after gel purification. As a control for 3' processing, ODN71 was radiolabelled and hybridized to AE117 lacking two nucleotides at the 3' end. For inhibition assays, 500 nM HIV-1 integrase and inhibitor were pre-incubated in reaction buffer (20 mM Hepes, pH 7.5, 5 mM DTT, 10 mM $MgCl_2$, 75 mM NaCl, 15% DMSO, 5% PEG 8000) for 30 min at 37°C. Then 10 nM 5'-labeled substrate was added, followed by incubation for 30 min at 37°C. The reaction was stopped by adding 1/5 loading buffer [95% (v/v) formamide, 20 mM EDTA, 0.005% (w/v) bromophenol blue] and heat inactivation at 90°C for 10 min. Samples were loaded on a 15% (19:1) denaturing polyacrylamide gel. The degree of inhibition was calculated with 100 × [1-(D-C)/(N-C)] where C, N and D were fractions of 3' processing products for DNA alone (C), DNA with integrase (N) and in addition of inhibitor (D), respectively.

Inhibition of HIV infection. The CXCR4-tropic HIV strain NL4/3 or VSV-G pseudotyped HIV-1 was used for TZM-bl cell infection. TZM-bl cells are HeLa cell derivatives, which present CD4 as well as the essential co-receptors CCR5 and CXCR4. These cells also produce HIV-1 LTR-driven luciferase expression cassette.[33] To investigate inhibition of HIV infection, 100 μl media, including 10^4 TZM-bl cells, were seeded into a 96-well plate. On the following day, medium was replaced with medium including different concentrations of aptamers. After incubation for 1 h, 80 μl of the medium was transferred into an extra well and 10 μl NL4/3 virus (1 ng/μl) were added to the cells. Cells were incubated for additional 6 h and, as a last step, previously transferred medium was added back to the cells. Forty-eight hours later, cell lysate luciferase activity was measured by Luciferase Assay System (Promega).

Cell viability assay. Oxidative processes of vital cells were detected via reduction of AlarmaBlue reagent (AbD Serotec), resulting in a reduced substance with characteristic absorption (570/600 nm). The assay was performed in 96-well plates with 10^4 cells in each 100 μl media. To detect proliferation, 20 μl AlarmaBlue reagent was added to each well, followed by 3 h of incubation.

Surface plasmon resonance. Aptamer-protein interactions were further analyzed by surface plasmon resonance (SPR) experiments using an SPR-2 Affinity Sensor (Sierra Sensors). A carboxymethylated sensor chip was pre-equilibrated with running buffer [1 × selection buffer, 0.01% (v/v) Tween] and activated by 0.1 M NHS (N-hydroxysuccinimide) and 0.4 M EDC [N-ethyl-N'-(3-dimethylaminopropyl) carbodimide] for the immobilization of the proteins on the chip surface. Hyper-IL-6 and IL-6, as a control, were immobilized on spot-1 and spot-2, respectively. After immobilization, non-reacted groups were inactivated by 1 M ethanolamine hydrochloride (pH 8.5). After generating a stable base line, a series of nucleic acids were tested by injecting each over both spots. The protein surface was regenerated using 0.1 M NaOH, followed by running buffer. Each signal from spot-2 was subtracted from the corresponding signal of spot-1, and the resulting curves were globally fitted to a 1:1 binding model using TraceDrawer software (Ridgeview Instruments).

Molecular dynamic simulations. Initial coordinates were constructed by simple modeling with UCSF chimera[34] using a published structure as the template.[18] These coordinates were supported by NMR spectroscopy and appeared stable in MD simulations.[18] The system was prepared with *LEaP*[35] (neutralization; octahedral periodic boundary conditions) resulting in final systems with approximately 10,000 water molecules. GROMACS[36] with the *parmbsc0*[37] force field was used for energy minimization and all simulations. All other parameters were set to published values[18] to allow comparison with literature results. After initial energy minimization (50,000 steps or gradient below 10^3 kJ $mol^{-1}nm^{-2}$), each system was subjected to position-restrained simulation with harmonic restraints on all heavy atoms for 0.1 ns (time step 0.2 fs). This was followed by 35 ns MD simulation weakly coupled to a heat bath (t = 300 K, τ = 0.1 ps) that was used for analysis.

Structural comparison of proteins. Structure searches for the non-sequence-related HIV-1 integrase (PDB acquisition codes 3LPT and 3LPU) and IL-6R (PDB 1N26) were performed with Salami,[38] Dali[39] and FATCAT.[40]

Outlook

The correlation between IL-6R binding and HIV-1 integrase inhibition of the selected aptamers remains unclear. Although many HIV integrase-inhibiting oligonucleotides have been described, their mode of action is not completely understood. Remarkably, cells that are infected with HIV express higher amounts of IL-6R on their cell surfaces or release increased amounts of soluble IL-6R.[49,50] Considering that IL-6R aptamers can be internalized,[15,51] a new inhibitory mechanism for these HIV inhibitors could be postulated. The inhibitors might enter the cell via IL-6R-mediated internalization and target HIV-1 integrase inside the cell. Whether this hypothesis holds and whether all IL-6R aptamers also inhibit HIV infection in vivo, will have to be investigated in future experiments. Accompanying structural investigations are under way.

Disclosure of Potential Conflicts of Interest

No potential conflicts of interest were disclosed.

Acknowledgments

We are grateful to Alina Wimmer and Frauke Fuchs for excellent technical assistance. This work is dedicated to Fritz Eckstein on the occasion of his 80th birthday.

Supplemental Materials

Supplemental materials may be found here:
www.landesbioscience.com/journals/rnabiology/article/22951

References

1. Tuerk C, Gold L. Systematic evolution of ligands by exponential enrichment: RNA ligands to bacteriophage T4 DNA polymerase. Science 1990; 249:505-10; PMID:2200121; http://dx.doi.org/10.1126/science.2200121.
2. Ellington AD, Szostak JW. In vitro selection of RNA molecules that bind specific ligands. Nature 1990; 346:818-22; PMID:1697402; http://dx.doi.org/10.1038/346818a0.
3. Robertson DL, Joyce GF. Selection in vitro of an RNA enzyme that specifically cleaves single-stranded DNA. Nature 1990; 344:467-8; PMID:1690861; http://dx.doi.org/10.1038/344467a0.
4. Holeman LA, Robinson SL, Szostak JW, Wilson C. Isolation and characterization of fluorophore-binding RNA aptamers. Fold Des 1998; 3:423-31; PMID:9889155; http://dx.doi.org/10.1016/S1359-0278(98)00059-5.
5. Blank M, Weinschenk T, Priemer M, Schluesener H. Systematic evolution of a DNA aptamer binding to rat brain tumor microvessels. selective targeting of endothelial regulatory protein pigpen. J Biol Chem 2001; 276:16464-8; PMID:11279054; http://dx.doi.org/10.1074/jbc.M100347200.
6. Lorger M, Engstler M, Homann M, Göringer HU. Targeting the variable surface of African trypanosomes with variant surface glycoprotein-specific, serum-stable RNA aptamers. Eukaryot Cell 2003; 2:84-94; PMID:12582125; http://dx.doi.org/10.1128/EC.2.1.84-94.2003.
7. Gellert M, Lipsett MN, Davies DR. Helix formation by guanylic acid. Proc Natl Acad Sci U S A 1962; 48:2013-8; PMID:13947099; http://dx.doi.org/10.1073/pnas.48.12.2013.
8. Sun H, Bennett RJ, Maizels N. The Saccharomyces cerevisiae Sgs1 helicase efficiently unwinds G-G paired DNAs. Nucleic Acids Res 1999; 27:1978-84; PMID:10198430; http://dx.doi.org/10.1093/nar/27.9.1978.
9. Greider CW, Blackburn EH. Identification of a specific telomere terminal transferase activity in Tetrahymena extracts. Cell 1985; 43:405-13; PMID:3907856; http://dx.doi.org/10.1016/0092-8674(85)90170-9.
10. Blackburn EH. The molecular structure of centromeres and telomeres. Annu Rev Biochem 1984; 53:163-94; PMID:6383193; http://dx.doi.org/10.1146/annurev.bi.53.070184.001115.
11. Kankia BI, Marky LA. Folding of the thrombin aptamer into a G-quadruplex with Sr(2+): stability, heat, and hydration. J Am Chem Soc 2001; 123:10799-804; PMID:11686680; http://dx.doi.org/10.1021/ja010008o.
12. Mashima T, Matsugami A, Nishikawa F, Nishikawa S, Katahira M. Unique quadruplex structure and interaction of an RNA aptamer against bovine prion protein. Nucleic Acids Res 2009; 37:6249-58; PMID:19666719; http://dx.doi.org/10.1093/nar/gkp647.
13. Murakami K, Nishikawa F, Noda K, Yokoyama T, Nishikawa S. Anti-bovine prion protein RNA aptamer containing tandem GGA repeat interacts both with recombinant bovine prion protein and its beta isoform with high affinity. Prion 2008; 2:73-80; PMID:19098441; http://dx.doi.org/10.4161/pri.2.2.7024.
14. Mann D, Reinemann C, Stoltenburg R, Strehlitz B. In vitro selection of DNA aptamers binding ethanolamine. Biochem Biophys Res Commun 2005; 338:1928-34; PMID:16289104; http://dx.doi.org/10.1016/j.bbrc.2005.10.172.
15. Meyer C, Eydeler K, Magbanua E, Zivkovic T, Piganeau N, Lorenzen I, et al. Interleukin-6 receptor specific RNA aptamers for cargo delivery into target cells. RNA Biol 2012; 9:67-80; PMID:22258147; http://dx.doi.org/10.4161/rna.9.1.18062.
16. Soundararajan S, Chen W, Spicer EK, Courtenay-Luck N, Fernandes DJ. The nucleolin targeting aptamer AS1411 destabilizes Bcl-2 messenger RNA in human breast cancer cells. Cancer Res 2008; 68:2358-65; PMID:18381443; http://dx.doi.org/10.1158/0008-5472.CAN-07-5723.
17. Ojwang JO, Buckheit RW, Pommier Y, Mazumder A, De Vreese K, Esté JA, et al. T30177, an oligonucleotide stabilized by an intramolecular guanosine octet, is a potent inhibitor of laboratory strains and clinical isolates of human immunodeficiency virus type 1. Antimicrob Agents Chemother 1995; 39:2426-35; PMID:8585721; http://dx.doi.org/10.1128/AAC.39.11.2426.
18. Li MH, Zhou YH, Luo Q, Li ZS. The 3D structures of G-quadruplexes of HIV-1 integrase inhibitors: molecular dynamics simulations in aqueous solution and in the gas phase. J Mol Model 2010; 16:645-57; PMID:19802725; http://dx.doi.org/10.1007/s00894-009-0592-0.
19. Ojwang J, Elbaggari A, Marshall HB, Jayaraman K, McGrath MS, Rando RF. Inhibition of human immunodeficiency virus type 1 activity in vitro by oligonucleotides composed entirely of guanosine and thymidine. J Acquir Immune Defic Syndr 1994; 7:560-70; PMID:7513761.
20. Jing N, Marchand C, Liu J, Mitra R, Hogan ME, Pommier Y. Mechanism of inhibition of HIV-1 integrase by G-tetrad-forming oligonucleotides in Vitro. J Biol Chem 2000; 275:21460-7; PMID:10801812; http://dx.doi.org/10.1074/jbc.M001436200.
21. Kelley S, Boroda S, Musier-Forsyth K, Kankia BI. HIV-integrase aptamer folds into a parallel quadruplex: a thermodynamic study. Biophys Chem 2011; 155:82-8; PMID:21435774; http://dx.doi.org/10.1016/j.bpc.2011.03.004.
22. Jing N, Hogan ME. Structure-activity of tetrad-forming oligonucleotides as a potent anti-HIV therapeutic drug. J Biol Chem 1998; 273:34992-9; PMID:9857031; http://dx.doi.org/10.1074/jbc.273.52.34992.
23. Esté JA, Cabrera C, Schols D, Cherepanov P, Gutierrez A, Witvrouw M, et al. Human immunodeficiency virus glycoprotein gp120 as the primary target for the antiviral action of AR177 (Zintevir). Mol Pharmacol 1998; 53:340-5; PMID:9463493.
24. Jones SA, Scheller J, Rose-John S. Therapeutic strategies for the clinical blockade of IL-6/gp130 signaling. J Clin Invest 2011; 121:3375-83; PMID:21881215; http://dx.doi.org/10.1172/JCI57158.
25. Stahl SJ, Zinn K. Nucleotide sequence of the cloned gene for bacteriophage T7 RNA polymerase. J Mol Biol 1981; 148:481-5; PMID:7310873; http://dx.doi.org/10.1016/0022-2836(81)90187-X.
26. Jostock T, Müllberg J, Ozbek S, Atreya R, Blinn G, Voltz N, et al. Soluble gp130 is the natural inhibitor of soluble interleukin-6 receptor transsignaling responses. Eur J Biochem 2001; 268:160-7; PMID:11121117; http://dx.doi.org/10.1046/j.1432-1327.2001.01867.x.
27. Fischer M, Goldschmitt J, Peschel C, Brakenhoff JP, Kallen KJ, Wollmer A, et al. I. A bioactive designer cytokine for human hematopoietic progenitor cell expansion. Nat Biotechnol 1997; 15:142-5; PMID:9035138; http://dx.doi.org/10.1038/nbt0297-142.
28. Mayer G, Wulffen B, Huber C, Brockmann J, Flicke B, Neumann L, et al. An RNA molecule that specifically inhibits G-protein-coupled receptor kinase 2 in vitro. RNA 2008; 14:524-34; PMID:18230760; http://dx.doi.org/10.1261/rna.821908.
29. Müller J, El-Maarri O, Oldenburg J, Pötzsch B, Mayer G. Monitoring the progression of the in vitro selection of nucleic acid aptamers by denaturing high-performance liquid chromatography. Anal Bioanal Chem 2008; 390:1033-7; PMID:17994225; http://dx.doi.org/10.1007/s00216-007-1699-8.
30. Lu M, Guo Q, Kallenbach NR. Thermodynamics of G-tetraplex formation by telomeric DNAs. Biochemistry 1993; 32:598-601; PMID:8422371; http://dx.doi.org/10.1021/bi00053a027.
31. Parissi V, Caumont AB, de Soultrait VR, Calmels C, Pichuantes S, Litvak S, et al. Selection of amino acid substitutions restoring activity of HIV-1 integrase mutated in its catalytic site using the yeast Saccharomyces cerevisiae. J Mol Biol 2000; 295:755-65; PMID:10656788; http://dx.doi.org/10.1006/jmbi.1999.3416.

32. Mazumder A, Cooney D, Agbaria R, Gupta M, Pommier Y. Inhibition of human immunodeficiency virus type 1 integrase by 3'-azido-3'-deoxythymidylate. Proc Natl Acad Sci U S A 1994; 91:5771-5; PMID:8016063; http://dx.doi.org/10.1073/pnas.91.13.5771.
33. Wei X, Decker JM, Liu H, Zhang Z, Arani RB, Kilby JM, et al. Emergence of resistant human immunodeficiency virus type 1 in patients receiving fusion inhibitor (T-20) monotherapy. Antimicrob Agents Chemother 2002; 46:1896-905; PMID:12019106; http://dx.doi.org/10.1128/AAC.46.6.1896-1905.2002.
34. Pettersen EF, Goddard TD, Huang CC, Couch GS, Greenblatt DM, Meng EC, et al. UCSF Chimera--a visualization system for exploratory research and analysis. J Comput Chem 2004; 25:1605-12; PMID:15264254; http://dx.doi.org/10.1002/jcc.20084.
35. Zhang W, Hou T, Schafmeister C, Ross WS, Case DA. LEaP and gleap. AmberTools Users' Manual Version 1.4: AMBER, 2010.
36. Van Der Spoel D, Lindahl E, Hess B, Groenhof G, Mark AE, Berendsen HJC. GROMACS: fast, flexible, and free. J Comput Chem 2005; 26:1701-18; PMID:16211538; http://dx.doi.org/10.1002/jcc.20291.
37. Pérez A, Marchán I, Svozil D, Sponer J, Cheatham TE 3rd, Laughton CA, et al. Refinement of the AMBER force field for nucleic acids: improving the description of alpha/gamma conformers. Biophys J 2007; 92:3817-29; PMID:17351000; http://dx.doi.org/10.1529/biophysj.106.097782.
38. Margraf T, Schenk G, Torda AE. The SALAMI protein structure search server. Nucleic Acids Res 2009; 37(Web Server issue):W480-4; PMID:19465380; http://dx.doi.org/10.1093/nar/gkp431.
39. Hasegawa H, Holm L. Advances and pitfalls of protein structural alignment. Curr Opin Struct Biol 2009; 19:341-8; PMID:19481444; http://dx.doi.org/10.1016/j.sbi.2009.04.003.
40. Ye Y, Godzik A. FATCAT: a web server for flexible structure comparison and structure similarity searching. Nucleic Acids Res 2004; 32(Web Server issue):W582-5; PMID:15215455; http://dx.doi.org/10.1093/nar/gkh430.
41. Jing N, Rando RF, Pommier Y, Hogan ME. Ion selective folding of loop domains in a potent anti-HIV oligonucleotide. Biochemistry 1997; 36:12498-505; PMID:9376354; http://dx.doi.org/10.1021/bi962798y.
42. Jing N, De Clercq E, Rando RF, Pallansch L, Lackman-Smith C, Lee S, et al. Stability-activity relationships of a family of G-tetrad forming oligonucleotides as potent HIV inhibitors. A basis for anti-HIV drug design. J Biol Chem 2000; 275:3421-30; PMID:10652335; http://dx.doi.org/10.1074/jbc.275.5.3421.
43. Mazumder A, Neamati N, Ojwang JO, Sunder S, Rando RF, Pommier Y. Inhibition of the human immunodeficiency virus type 1 integrase by guanosine quartet structures. Biochemistry 1996; 35:13762-71; PMID:8901518; http://dx.doi.org/10.1021/bi960541u.
44. Joachimi A, Benz A, Hartig JS. A comparison of DNA and RNA quadruplex structures and stabilities. Bioorg Med Chem 2009; 17:6811-5; PMID:19736017; http://dx.doi.org/10.1016/j.bmc.2009.08.043.
45. Varghese JN, Moritz RL, Lou MZ, Van Donkelaar A, Ji H, Ivancic N, et al. Structure of the extracellular domains of the human interleukin-6 receptor alpha -chain. Proc Natl Acad Sci U S A 2002; 99:15959-64; PMID:12461182; http://dx.doi.org/10.1073/pnas.232432399.
46. Christ F, Voet A, Marchand A, Nicolet S, Desimmie BA, Marchand D, et al. Rational design of small-molecule inhibitors of the LEDGF/p75-integrase interaction and HIV replication. Nat Chem Biol 2010; 6:442-8; PMID:20473303; http://dx.doi.org/10.1038/nchembio.370.
47. Lauhon CT, Szostak JW. RNA aptamers that bind flavin and nicotinamide redox cofactors. J Am Chem Soc 1995; 117:1246-57; PMID:11539282; http://dx.doi.org/10.1021/ja00109a008.
48. Walsh R, DeRosa MC. Retention of function in the DNA homolog of the RNA dopamine aptamer. Biochem Biophys Res Commun 2009; 388:732-5; PMID:19699181; http://dx.doi.org/10.1016/j.bbrc.2009.08.084.
49. Honda M, Yamamoto S, Cheng M, Yasukawa K, Suzuki H, Saito T, et al. Human soluble IL-6 receptor: its detection and enhanced release by HIV infection. J Immunol 1992; 148:2175-80; PMID:1545125.
50. Novick D, Shulman LM, Chen L, Revel M. Enhancement of interleukin 6 cytostatic effect on human breast carcinoma cells by soluble IL-6 receptor from urine and reversion by monoclonal antibody. Cytokine 1992; 4:6-11; PMID:1617157; http://dx.doi.org/10.1016/1043-4666(92)90029-Q.
51. Zhou J, Rossi JJ. Cell-specific aptamer-mediated targeted drug delivery. Oligonucleotides 2011; 21:1-10; PMID:21182455; http://dx.doi.org/10.1089/oli.2010.0264.
52. Hazel P, Huppert J, Balasubramanian S, Neidle S. Loop-length-dependent folding of G-quadruplexes. J Am Chem Soc 2004; 126:16405-15; PMID:15600342; http://dx.doi.org/10.1021/ja045154j.